http://dx.doi.org/10.21577/0103-5053.20170218

J. Braz. Chem. Soc., Vol. 29, No. 6, 1225-1236, 2018
Printed in Brazil - ©2018 Sociedade Brasileira de Química

Article

Synthesis of Chelating Agent Free-Solid Phase Extractor (CAF-SPE) Based on New $SiO_2/Al_2O_3/SnO_2$ Ternary Oxide and Application for Online Preconcentration of Pb^{2+} Coupled with FAAS

César R. T. Tarley,[a,b] Guilherme L. Scheel,[a] Emerson S. Ribeiro,[c,d] Caroline D. Zappielo[a] and Fabio A. C. Suquila[a]*

[a]*Departamento de Química, Universidade Estadual de Londrina (UEL), 86051-990 Londrina-PR, Brazil*

[b]*Instituto Nacional de Ciência e Tecnologia (INCT) em Bioanalítica, Departamento de Química Analítica, Instituto de Química, Universidade Estadual de Campinas (UNICAMP), 13083-970 Campinas-SP, Brazil*

[c]*Grupo LaDANM, Instituto de Química, Universidade Federal do Rio de Janeiro (UFRJ), 21941-909 Rio de Janeiro-RJ, Brazil*

[d]*Instituto Nacional de Tecnologias Alternativas para Detecção, Avaliação Toxicológica e Remoção de Micropoluentes e Radioativos (INCT-DATREM), Instituto de Química, Universidade Estadual Paulista (Unesp), CP 355, 14800-900 Araraquara-SP, Brazil*

A new online solid phase preconcentration method using the new $SiO_2/Al_2O_3/SnO_2$ ternary oxide (designated as SiAlSn) as chelating agent free-solid phase extractor (CAF-SPE) coupled to flame atomic absorption spectrometry (FAAS) for Pb^{2+} determination at trace levels in different kind of samples is proposed. The solid adsorbent has been characterized by Fourier transform infrared spectroscopy (FTIR), scanning electron miscroscopy (SEM), energy dispersive X-ray spectroscopy (EDS), X-ray fluorescence spectroscopy (XRF) and textural data. The method involves the preconcentration using time-based sampling of Pb^{2+} solution at pH 4.3 through 100.0 mg of packed adsorbed into a mini-column under flow rate of 4.0 mL min^{-1} during 5 min. The elution step was accomplished by using 1.0 mol L^{-1} HCl. A wide range of analytical curve (5.0-400.0 μg L^{-1}), high enrichment factor (40.5), low consumption index (0.5 mL) and low limits of quantification and detection, 5.0 and 1.5 μg L^{-1}, respectively, were obtained with the developed method. Practical application of method was tested on water samples, chocolate powder, *Ginkgo biloba* and sediment (certified reference material). On the basis of the results, the SiAlSn can be considered an effective adsorbent belonging to the class of CAF-SPE for Pb^{2+} determination from different matrices.

Keywords: lead, online solid phase extraction, $SiO_2/Al_2O_3/SnO_2$, flame atomic absorption spectrometry, food and water samples

Introduction

Lead contamination has been considered one of the most environmental concern worldwide due to numerous acute and chronic adverse effects caused by the element.[1,2] To the population in general, which is not occupationally exposed, water and food are significant sources of exposure to lead.[2] The most common lead contamination pathways to water are the household plumbing corrosion and anthropic pollution, while to food are the development of plants grown in soil containing high amount of lead and the accidental additive picked up during food processing.[3-6] Due to its high degree of toxicity and the effects caused to the ecosystem, a rigid monitoring of the activities involving this metal is required.

According to World Health Organization (WHO),[6-8] the health-based guideline established value for lead in drinking water is 10.0 μg L^{-1}, while for food, the seventy-third report of the Joint Food Agriculture Organization/WHO Expert Committee on Food Additives estimated the mean dietary

*e-mail: ctarleyquim@yahoo.com.br

exposure *per* day and body weight for children (aged about 1-4 years) and to adults being in the range 0.03-9.00 and 0.02-3.00 μg kg^{-1}, respectively. The Brazilian Ministry of Health[9] and CONAMA resolution No. 357 (Brazil National Environment Council)[10] established the maximum allowable lead content in freshwater as 30.0 μg L^{-1}, while for drinking water this index reduces to 10.0 μg L^{-1} and effluents released into aquatic bodies the concentration is 500.0 μg L^{-1}. With regard to food samples, the Brazilian Ministry of Health[11] established maximum limits of lead between 0.01-2.00 mg kg^{-1} to different types of foodstuffs. According to those strict regulations, the development of analytical methods to determine trace amounts of lead is extremely essential.

Flame atomic absorption spectrometry (FAAS) and graphite furnace atomic absorption spectrometry (GFAAS) have been widely used for determining lead ions.[8,12] In general, among the spectrometric techniques, the FAAS stands out in relation to the others for being a simple, selective, easy-to-operate technique with a high analytical frequency and mainly because it exhibits low maintenance and acquisition costs.[8,12,13] However, the low sensitivity makes it unsuitable for lead quantification at trace levels in different samples.[14] To overcome this limitation, preconcentration procedures before quantification are usually required.[15] Preconcentration methods based on online solid phase extraction (SPE) are very useful due to their simplicity, high enrichment factor, reduced reagent consumption, accuracy, high analytical frequency and easy regeneration of the solid phase adsorbent. Such characteristics relies to the choice of a material with high chemical and mechanical stability and high adsorption capacity.[16,17]

Among the solid phase adsorbents, silica gel (SiO_2) matrix is widely utilized due to its high mechanical stability at high pressure and low swellability in different solvents. However, silica-based materials have chemical limitations regarding the adsorptive capacity against metallic ions, as well as low chemical stability in high acid and/or high alkaline media.[18] Regarding those traditional polymeric phases such as polyurethane, amberlite XAD and modified octadecylsilica, the surface modification with chelating agents has been a strategy for improving the performance of these solid phase extractor towards metal ions adsorption.[19-21] On the other hand, these materials usually present low reusability as result of loss of chelating agents after several preconcentration/elution cycles. In this sense, the synthesis of chelating agent free-solid phase extractor (CAF-SPE) based on mixed oxides grafted into a silica matrix has been an interesting strategy for obtaining new materials with high surface area, high resistance to acids and bases, high reusability and improvements on the sensitivity and selectivity towards metal ions adsorption.[22-24]

Grafting by sol-gel process has been the choice method for the preparation of hybrid material ($SiO_2/M_xO_y = Al_2O_3$, TiO_2, ZrO_2, Nb_2O_5, SnO_2) due to the uniform dispersion of metallic oxides in the matrix.[18,25,26] Furthermore, the Lewis and/or Brønsted acid sites on the surface of mixed oxides makes them interesting materials for various applications, including preconcentration of metallic ions and anions.[27,28] Al_2O_3 and SnO_2 are amphoteric oxides, allowing them to react with both acids and bases,[29] and SnO_2 exhibits Lewis and Brønsted acid sites.[30,31] Therefore, acid-base interactions with lead ions (Pb^{2+}) and binding sites of hybrid material are expected.[32]

Bearing in mind the great potential of hydrid materials based on SiO_2/M_xO_y as chelating agent free-solid phase extractor, as well as their few analytical application, this study deals with synthesizing a new $SiO_2/Al_2O_3/SnO_2$ ternary oxide (designated as SiAlSn) obtained by sol-gel process and its evaluation as adsorbent for Pb^{2+} preconcentration using an online SPE system coupled to FAAS. The effectiveness of the SiAlSn was investigated by comparing with the Pb^{2+} preconcentration on an unmodified SiO_2 matrix.

Experimental

Apparatus

The online preconcentration experiments with mini-column were coupled with a flame atomic absorption spectrometer (FAAS) Shimadzu® AA-7000 (Tokyo, Japan) equipped with a lead hollow-cathode lamp as radiation source (wavelength, 217.0 nm; current, 10 mA), a deuterium lamp for background correction and a flame composition operated with acetylene at flow rate of 2.0 L min^{-1} and air flow rate of 15.0 L min^{-1}. The flow injection system was constructed by an Ismaltec® IPC-08 peristaltic pump (Glattbrugg, Switzerland), Tygon® tubes (Courbevoie, France), polyethylene tubes (to propel sample solutions; diameter, 0.8 mm) and a homemade poly(methyl methacrylate) injector-commutator. The sample pH was measured with a Metrohm® 827 pH lab digital pH meter (Herisau, Switzerland). Infrared spectra were recorded by using a Shimadzu® 8300 Fourier transform infrared spectrophotometer (FTIR, Tokyo, Japan) in trasmission mode and range of 4000-400 cm^{-1} (through a conventional KBr pellet technique). The material surface morphology was evaluated by a scanning electron microscopy (SEM) using a JEOL® JSM 6360-LV equipment (Tokyo, Japan) with probe of energy dispersive

spectroscopy (EDS). Before microscopy analysis, the material had been previously coated with a gold thin layer using a sputter coater Leica® Bal-Tec Med 020 (Wetzlar, Germany). Micrographs were obtained by applying an electron acceleration voltage of 20 kV. The SiO_2, Al_2O_3 and SnO_2 contents in the SiAlSn were determined by using X-ray fluorescence (XRF) on a PANalytical®Axios mAX (Almelo, the Netherlands). To determine the specific surface area, average pore diameter and pore volume, a surface area and pore size analyzer Quantachrome® Nova Model 1200e (Boynton Beach, USA) automatic nitrogen gas adsorption instrument was utilized. The specific surface area was estimated from nitrogen adsorption isotherms according to the Brunauer-Emmett-Teller (BET) multipoint method and the average pore diameter as well the pore volume were determined through the Barrett-Joyner-Halenda (BJH) method after the sample preheating at 120 °C by 4 h under vacuum. Certified reference material, herbal medicine and chocolate powder were decomposed in a Milestone Inc® Ethos Plus microwave oven (Sorisole, Italy).

Reagents and solutions

The SiAlSn synthesis was accomplished by using tetraethylorthosilicate (TEOS, $Si(OC_2H_5)_4$, 98%), aluminum isopropoxide ($Al[OCH(CH_3)_2]_3$, 98%), tin(IV) chloride pentahydrate ($SnCl_4{\cdot}5H_2O$, 98%), trifluoroacetic acid (CF_3COOH, 99%), all purchased from Sigma-Aldrich (Saint Louis, MO, USA). Ethanol (EtOH, 99.8%), hydrochloric acid (HCl, 37% v/v) and nitric acid (HNO_3, 95% v/v) were purchased from Vetec® (Duque de Caxias, RJ, Brazil). To prevent any possible contamination, all glassware was kept in a 10% (v/v) HNO_3 solution for 24 h with posterior cleaning with ultra-pure water. Aqueous solutions were prepared utilizing ultrapure water from a Millipore® Milli-Q System (Billerica, MA, USA). The 1000 mg L^{-1} Pb^{2+} standard solution was purchased from Merck® (Darmstadt, Germany) and the working solutions were properly diluted with ultrapure water. Britton-Robinson and acetate buffer solutions were prepared from respective sodium salts, made from analytical grade reagents without previous purification. To interference study, solutions of Co^{2+}, Zn^{2+}, Ni^{2+}, Cu^{2+}, Cd^{2+}, As^{3+}, Na^{+}, Ca^{2+}, Ba^{2+} and Mg^{2+} were prepared from their standard solutions (1000 mg L^{-1}) from Quimilab® (Jacareí, SP, Brazil) or from their salts (analytical grade). The solution pH values were adjusted with HCl and/or sodium hydroxide (NaOH) solutions, made from analytical grade reagents. Also, HCl solution was utilized to elute the target metal from the mini-column. Analytical grade hydrogen peroxide (H_2O_2, 30% v/v) from Synth® (Diadema, SP, Brazil), fluoridric acid (HF, 40% v/v) from Nuclear® (Diadema, SP, Brazil), HCl and HNO_3 were utilized to decompose chocolate powder, *Ginkgo biloba* and certified reference material sample. The certified reference material (Marine sediment, MESS-3) was provided by National Research Council of Canada (Ottawa, Canada).

Synthesis of $SiO_2/Al_2O_3/SnO_2$ ternary oxide

The synthesis of SiAlSn was performed by means of sol-gel process. To promote TEOS prehydrolysis, 230.0 mL of TEOS:EtOH (1:1, v/v) solution was added with 13.0 mL of 3.5 mol L^{-1} HCl in a reactor and kept under agitation for 3 h under 70 °C. Before gelification, in the solution it was added 50.0 mL of an ethanolic solution containing 23.28 g $SnCl_4{\cdot}5H_2O$, 20.5 g of $Al[OCH(CH_3)_2]_3$ dissolved in 20.0 mL of CF_3COOH and 25.0 mL of 3.0 mol L^{-1} HNO_3 dropwise. The mixture was kept under agitation at 70 °C until total gelification.

Thereafter, the gel was submitted to a drying step in order to obtain the xerogel. The gel was transferred to a beaker and heated at 80 °C initially in a hot plate, and after into a drying oven until the complete solvent evaporation. Subsequently, the material was carefully powdered, dried by 4 h in vaccum at 80 °C and submitted by 6 h into a Soxhlet system with ethanol to remove the reagents excess and purification. The material was also washed multiple times with 0.1 mol L^{-1} HNO_3, ethanol and ultrapure water. Lastly, the material was submitted by 2 h at 80 °C in a vacuum for total dryness.

Online preconcentration procedure coupled with FAAS

The online preconcentration procedure was accomplished by percolating Pb^{2+} solution buffered with 0.1 mol L^{-1} acetate buffer (pH 4.3) through a home-made cylindrical polyethylene mini-column (5.5 × 0.8 cm i.d.) packed with 100.0 mg of SiAlSn under a flow rate of 4.0 mL min^{-1} during 5 min. Cotton tissues were fixed between the mini-column cylindrical body and its conical sides in order to maintain the material inside. After the preconcentration, the switch to elution step was made manually and the Pb^{2+} ions were desorbed with 1.0 mol L^{-1} HCl in counter current at a flow rate of 4.0 mL min^{-1} toward the FAAS detector.

Optimization procedure

The online preconcentration procedure was optimized by applying Doehlert design for three variables (pH,

Britton-Robinson buffer concentration and preconcentration flow), totaling thirteen experiments. At central point the assay was done in triplicate to estimate the experimental error. The pH was varied into seven levels in the range of 3.0-9.0, buffer concentration was varied into five levels in the range of 0.0525-0.1800 mol L^{-1} with Britton-Robinson buffer, and preconcentration flow was varied into three levels in the range of 2.0-6.0 mL min^{-1}. The volume and concentration of Pb^{2+} ions, type and concentration of eluent, adsorbent mass and elution flow rate were previously fixed in 20.0 mL, 200.0 μg L^{-1} Pb^{2+}, 1.0 mol L^{-1} HCl, 100.0 mg and 4.0 mL min^{-1}, respectively. The sequence of the experiments was carried out randomly. Subsequently the buffer nature was analyzed in a univariate manner, in triplicate.

Interference study

To evaluate the Pb^{2+} preconcentration by SiAlSn in the presence of possible interfering ions, binary solution of Co^{2+}, Zn^{2+}, Ni^{2+}, Cu^{2+}, Cd^{2+}, As^{3+}, Na^{+}, Ca^{2+}, Ba^{2+} or Mg^{2+} with the target metal were subjected to the online preconcentration procedure, under optimized conditions. The Pb^{2+} concentration was fixed in 200.0 μg L^{-1} and the studied proportions (m/m) of the target metal and potential interfering ions were 1:1, 1:5, 1:10, 1:50 and/or 1:100. The interference effect was estimated by the Pb^{2+} recovery percentage, defined as the ratio between the analytical responses in the presence and absence of co-existing ions.

Determination of figures of merit

Under optimized conditions, the analytical performance of the method was analyzed by enrichment factor (EF), concentration efficiency (CE), consumption index (CI), analytical frequency (AF), limit of quantification (LOQ) and detection (LOD), range of analytical curve, inter/intraday precision and accuracy. All figures of merit were determined according to the international regulation[33] and/or according to literature.[34-36] The range of analytical curve obtained by using the preconcentration method was constructed in the range 5.0-400.0 μg L^{-1}. The EF was calculated as the ratio of the slope of the linear regression models of Pb^{2+} concentration obtained with and without preconcentration step. The CE was obtained by the ratio between the EF and the time spent to preconcentrate the sample (5 min). CI was calculated by the ratio between the sample volume submitted to preconcentration (20.0 mL) and EF. AF was given with the division of 1 h by the time consumed to realize preconcentration and elution of Pb^{2+} ions. LOD and LOQ were determined by using absorbance values of blank solutions. The LOD and LOQ were calculated by using the ratio of three and ten times the standard deviation, respectively, of ten blank samples divided by the slope of the linear regression. Inter/intraday precision were calculated with three Pb^{2+} standard solutions at 5.0, 100.0 and 400.0 μg L^{-1} concentrations. The relative standard deviations (RSD, %) were calculated to determine the precision. Accuracy was assessed by analysis of certified reference material.

Real samples and reference material preparation

To evaluate the applicability of proposed method, water (mineral, tap and lake water), herbal medicine (*Ginkgo biloba*) and chocolate powder samples were analyzed. Tap water and lake water were collected at Londrina State University and Lake Igapó III, respectively, both located in Londrina, Paraná, Brazil. Before analysis, lake water sample was acidified until pH 2.0 with HNO_3 solution and filtered through a 0.45 μm cellulose acetate membrane. *Ginkgo biloba* powder, chocolate powder and mineral water samples were obtained from local supermarket. The microwave-assisted digestion of 700.0 and 500.0 mg of *Ginkgo biloba* and chocolate powder samples, respectively, was carried out by using 10.0 mL of concentrated HNO_3 and 4.0 mL of 30% (v/v) H_2O_2. The heating program was accomplished by setting 1200 W of nominal power with a linear temperature gradient. The temperature gradient was performed as follows: heating to 80 °C, 0.00-6.00 min; plateau at 80 °C, 6.01-11.00 min; heating to 120 °C, 11.01-18.00 min; plateau at 120 °C, 18.01-23.00 min; heating to 210 °C, 23.01-38.00 min; plateau at 210 °C, 38.01-58.00 min. After sample digestion, the samples were heated on a hot plate to near dryness, to eliminate the residual HNO_3, and then cooled to room temperature. Then, the acetate buffer (pH 4.3) was added. Blank solutions were prepared for each sample.

The accuracy was checked by analysis of certified reference material MESS-3. Aliquots of 200.0 mg of MESS-3 were weighted into polytetrafluoroethylene flasks and decomposed overnight with 10.0 mL of Lefort aqua regia solution (HNO_3:HCl, 3:1, v/v) and 1.0 mL of HF. Subsequently, the mixture was subjected to microwave digestion using a fixed nominal power of 700 W and a linear temperature gradient. The temperature gradient was performed as follows: heating to 120 °C, 0.00-15.00 min; plateau at 120 °C, 15.01-25.00 min; heating to 200 °C, 25.01-45.00 min; plateau at 200 °C, 45.01-60.00 min; heating to 220 °C, 60.01-75.00 min. To decrease the pressure and refrigerate the digested samples, 30 min of exhaustion time were required.

Afterwards, the samples were heated on a hot plate to near dryness, to eliminate the residual HNO_3, and then cooled to room temperature. Then, the acetate buffer (pH 4.3) was added. Blank solutions were prepared for each sample.

Computational programs

To perform the Doehlert matrix design, the responses surfaces representations and the optimum conditions the experimental data were processed with the software Statistica 7.0.[37] The others graphical representations were made utilizing the software Origin Pro 8 SR0.[38]

Results and Discussion

Characterization of $SiO_2/Al_2O_3/SnO_2$ ternary oxide

The surface morphology of the SiAlSn was analyzed by SEM (Figure 1). As observed in Figure 1a, the SiAlSn presented a flat or rough surface with irregular and non-spherical particles smaller than 50 μm. Such morphological feature was somewhat expected, which is very common for mixed oxides obtained by the sol-gel process. In spite of irregular size and non-spherical particles, it has been observed that SiAlSn is attractive as column packing material for flow injection system, since no overpressure into the column, leakages and low repeatability of measurements was observed. One should note that, the presence of roughness on the surface of material can facilitate mass transfer and provides an increase in the surface area.[39,40]

In order to obtain a rough estimation of mass percentages of the components and the dispersion of aluminium and tin in the surface of material, EDS spectrum (data not shown) and elemental mapping were recorded, respectively.

From EDS spectrum of SiAlSn (data not shown), it was found percentages of O (70.00 wt.%), Si (25.46 wt.%), Al (1.71 wt.%) and Sn (2.82 wt.%); obtaining an atomic molar ratio of Si/Al = 14.3 and Si/Sn = 38.2. From the EDS images (Figure 2), no phase segregation or oxide particle islands were observed with the studied magnification, showing highly dispersed metal oxides due to strong covalent bonding interaction with the siloxane groups in the silica matrix. This high dispersion is extremely important because it alters positively the number of sites on the material surface and facilitates the access to the binding sites.[39,40] The obtained results by XRF for the SiO_2, Al_2O_3 and SnO_2 amounts incorporated in the SiAlSn, were 87.22, 3.08 and 9.69 wt.%, respectively. The atomic molar ratios were Si/Al = 13.6 and Si/Sn = 38.1, thus corroborating with the EDS analysis and showing that the atomic distribution on the surface (EDS analysis) as in the bulk of the material (XRF analysis) is the same.

From the FTIR spectra, some characteristic functional groups of the SiAlSn were observed and compared with net silica spectrum (Figure 3). The wide absorption band at 3460 cm^{-1} corresponds to OH stretching vibrations due to the presence of silanol groups in the silica matrix and/or adsorbed water presented due to hydrogen bonds. Also, the band presented at 1656 cm^{-1} can be attributed to the angular deformation vibration of adsorbed water, confirming the presence of these molecules on the material surface.[41,42] A wide shoulder band containing the bands at 1201 and 1067 cm^{-1} was observed in both spectra, which can be attributed to Si–O–Si asymmetric stretching vibration, while the band at 800 cm^{-1} corresponds to the symmetrical stretching. Si–O–Si angular deformation vibrations are evidenced at 571 and 453 cm^{-1}.[43-45] The band at 917 cm^{-1} can be attributed to Si–OH angular deformation vibration. From the bands definition and the similarity between the spectra, it can be inferred that the SiO_2 network is only

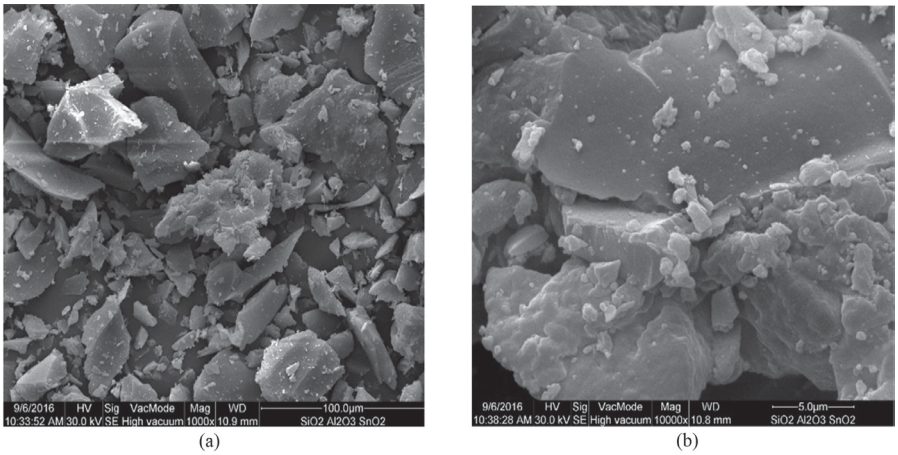

(a) (b)

Figure 1. SEM images for the SiAlSn (a) 1,000 times magnification and (b) 10,000 times magnification.

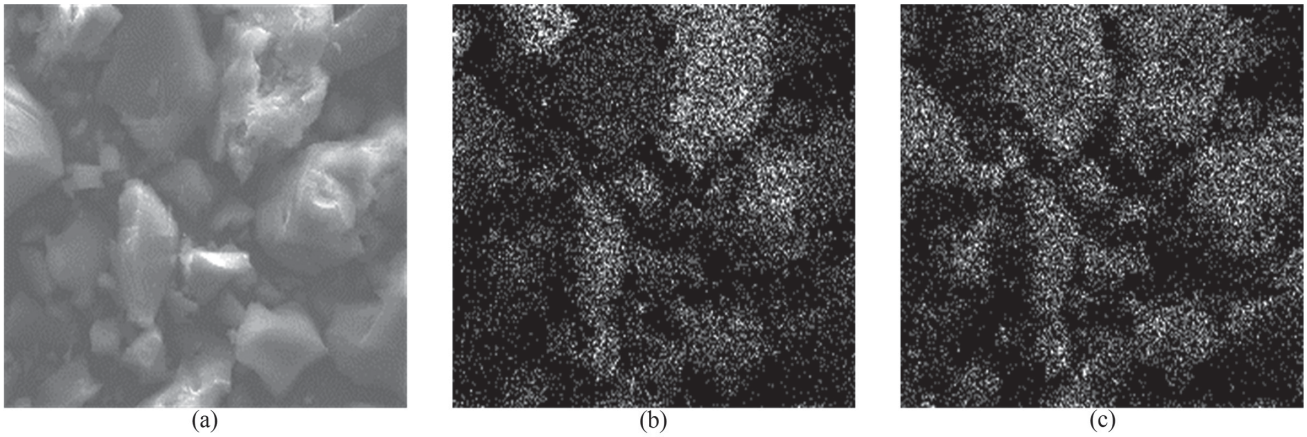

Figure 2. (a) SEM image of various particles from SiAlSn and its corresponding EDS images to (b) aluminum and (c) tin. Condition: scale of 80 μm.

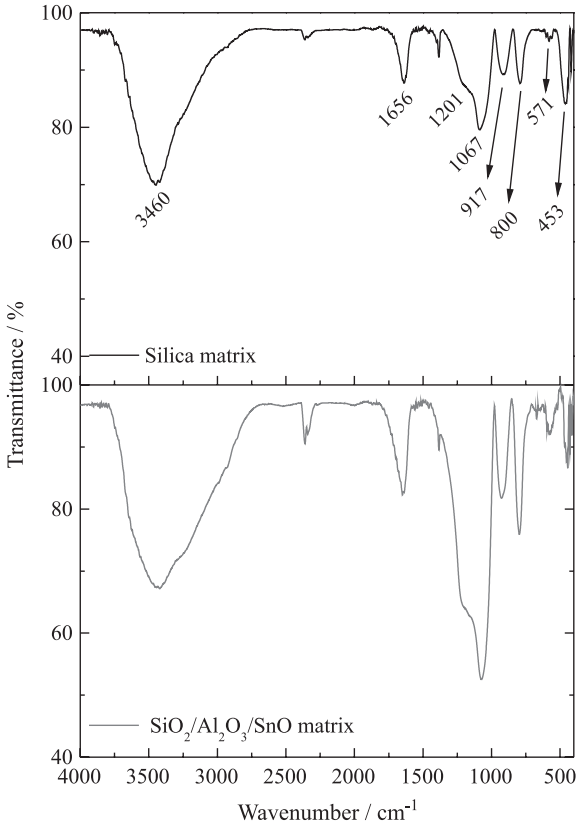

Figure 3. FTIR spectra of silica matrix (upper) and SiAlSn (bottom).

slightly disturbed by the incorporation of the metal oxides Al_2O_3 and SnO_2, suggesting a good dispersion of the both in the silica matrix, as observed from the EDS data.

The textural parameters of SiAlSn material were determined from nitrogen adsorption-desorption isotherm and the obtained results were compared with silica matrix results previously reported in literature.[39] The adsorption isotherm showed no hysteresis (Figure 4a) and its concave format indicates that the amount adsorbed approaches a limiting value. This limiting uptake is governed by the accessible pore volume rather than by the internal surface area. This type of isotherm, which is of type I, is very common in materials having pore size distributions over a broader range, including narrow mesopores and small external surfaces.[46] From BET and BJH data, the surface area, pore volume and pore diameter were found to be 416.9 $m^2\ g^{-1}$, $1.83 \times 10^{-2}\ cm^3\ g^{-1}$ and 3.37 nm, respectively. According to the pore distribution obtained by the BJH method (Figure 4b), it is observed the predominance of pores with a diameter of 3.37 nm, thus suggesting that the concave isotherm behavior is attributed to the narrow mesopores. The obtained textural data to the material were significantly higher when compared to those of the pure silica matrix (220.0 $m^2\ g^{-1}$, $1.14 \times 10^{-2}\ cm^3\ g^{-1}$ and 1.57 nm for surface area, volume and average pore diameter, respectively), being of paramount importance to increase the capacity of Pb^{2+} ions to diffuse through the pores and their accessibility to the active sites of the adsorbent.[18,44]

Optimization

The best working conditions for adsorption of Pb^{2+} ions on SiAlSn were determined using a three-variables Doehlert design associated with response surface methodology. Table 1 presents the three-variables Doehlert design containing the codified levels, the parameters variation values (in parenthesis) and the obtained absorbance responses from each assay. The absorbance responses obtained were utilized to construct the model equation and the response surfaces. The significance of model statistical was evaluated by analysis of variance (ANOVA). The quadratic regression model (equation 1) establishes the relationship between the buffer concentration (BC), pH, preconcentration flow (PRF) and the absorbance. The model variation is explained by 94.5% and the regression coefficients by 98.0% at a 95% confidence level.

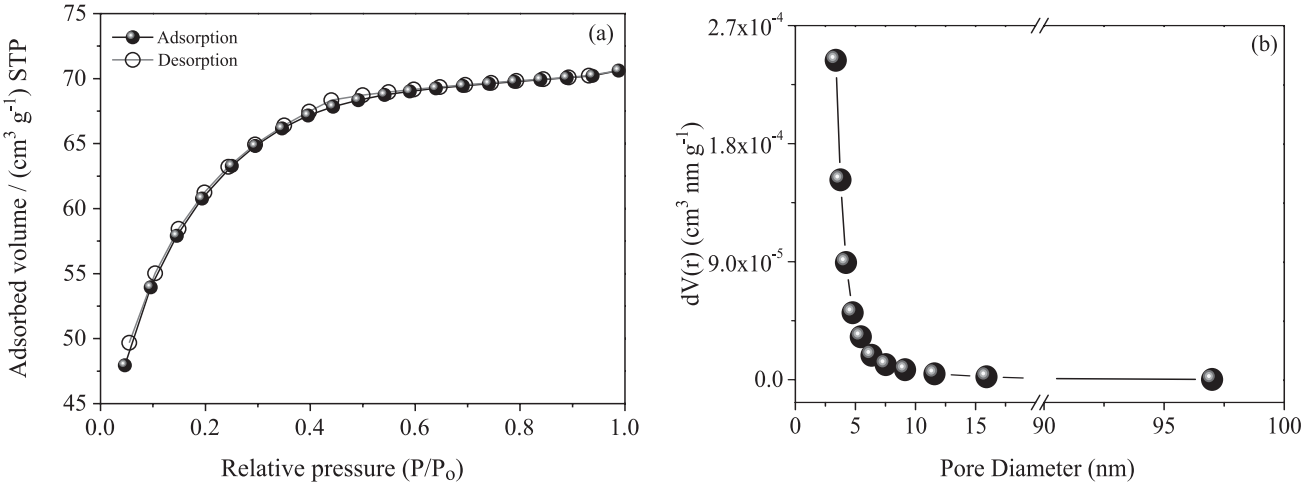

Figure 4. (a) Nitrogen adsorption-desorption isotherm and (b) BJH pore size distribution. For experimental detail, see Apparatus section.

Table 1. Doehlert matrix optimization and the obtained responses to online preconcentration procedure of Pb^{2+} using SiAlSn as solid phase adsorbent

Assay	pH	BC / (mol L^{-1})	PRF / (mL min^{-1})	Absorbance
1	0 (6.00)	0 (0.0950)	0 (4.00)	0.365/0.342/0.350
2	0 (6.00)	1 (0.1800)	0 (4.00)	0.060
3	0.866 (9.00)	0.5 (0.1375)	0 (4.00)	0.156
4	0.289 (7.00)	0.5 (0.1375)	0.817 (6.00)	0.088
5	0 (6.00)	–1 (0.0100)	0 (4.00)	0.041
6	–0.866 (3.00)	–0.5 (0.0525)	0 (4.00)	0.250
7	–0.289 (5.00)	–0.5 (0.0525)	–0.817 (2.00)	0.139
8	–0.866 (3.00)	0.5 (0.1375)	0 (4.00)	0.270
9	–0.289 (5.00)	0.5 (0.1375)	–0.817 (2.00)	0.280
10	0.866 (9.00)	–0.5 (0.0525)	0 (4.00)	0.123
11	0.577 (8.00)	0 (0.0950)	–0.817 (2.00)	0.124
12	0.289 (7.00)	–0.5 (0.0525)	0.817 (6.00)	0.075
13	–0.577 (4.00)	0 (0.0950)	0.817 (6.00)	0.083

BC: buffer concentration; PRF: preconcentration flow. The values in parenthesis are the parameters variation.

$$\text{Absorbance} = (-0.536 \pm 0.075) + (0.021 \pm 0.015)\,\text{pH} - (0.009 \pm 0.001)\,\text{pH}^2 + (9.702 \pm 0.439)\,\text{BC} - (41.776 \pm 1.475)\,\text{BC}^2 + (0.227 \pm 0.019)\,\text{PRF} - (0.038 \pm 0.002)\,\text{PRF}^2 + \mathbf{(0.025 \pm 0.046)\,pH \times BC} + (0.015 \pm 0.002)\,\text{pH} \times \text{PRF} - (0.382 \pm 0.072)\,\text{BC} \times \text{PRF} \quad (1)$$

The mentioned statistical model allows to observe the non significance of the positive regression coefficient value to the interaction between pH and BC (equation 1, in bold) because of its standard error being superior. According to ANOVA, the lack of fit was not statistically significant since the value of 8.17 obtained by the ratio between the lack of fit quadratic mean and pure error quadratic mean was smaller than the tabulated *F*-distribution value ($F_{3,2}$) of 19.16, at a 95% confidence level. Analyzing the responses surfaces (Figure 5), maximum points were observed, indicating optimum conditions to all variables. To obtain the optimum conditions through these surfaces, it was necessary to derive the equation obtained from the design in function of the chosen variable and equalize it to zero. However, the same results can be obtained by processing the data in statistical software, as performed in this work.[47,48] The obtained optimum conditions values to BC, pH and PRF were 0.1 mol L^{-1}, 4.3 and 3.3 mL min^{-1}, respectively. To PRF the adopted condition was 4.0 mL min^{-1} to increase the analytical frequency, instead of the optimum condition.

Interference studies

The competition effect of Pb^{2+} ions with other ions in the preconcentration system was evaluated from the preconcentration of binary mixtures containing a fixed

amount of the target metal and interfering ion in different proportion, under optimized condition. As can be seen in Figures 6, the interfering ions presence caused a relative error of ± 15 around the total recovery. Even at higher concentrations of interfering ions, the preconcentration of lead ions onto SiAlSn was observed to be very tolerant.

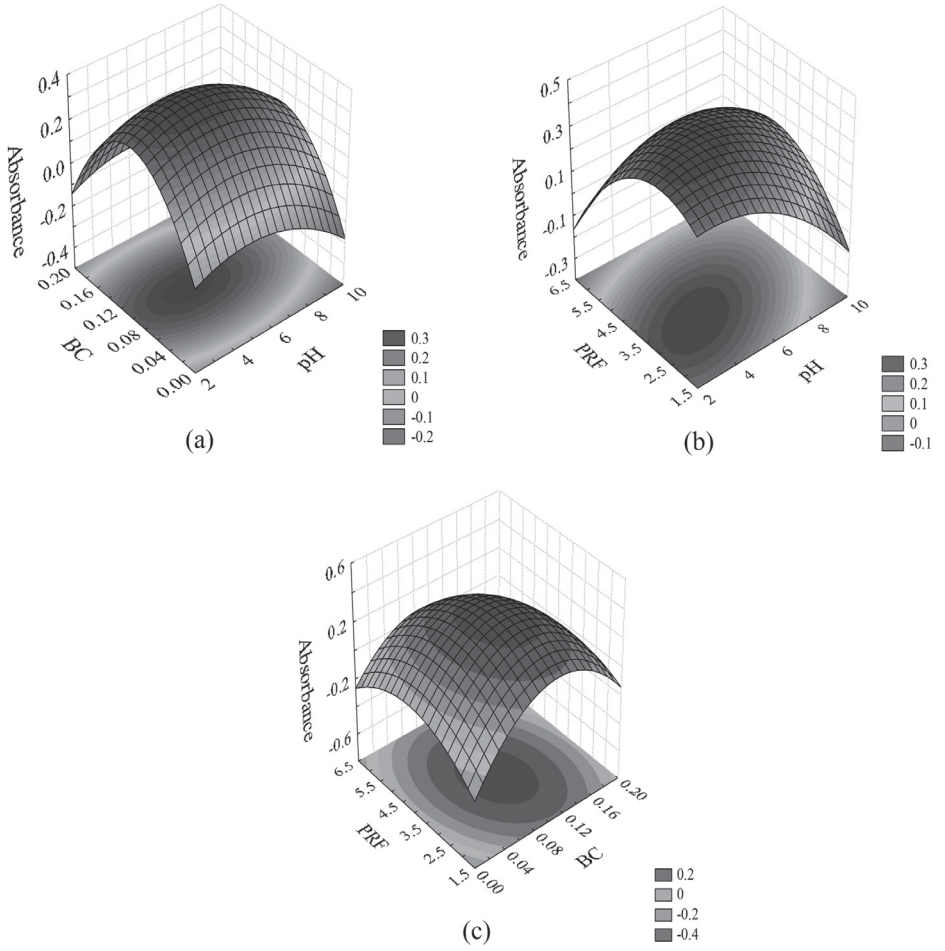

Figure 5. Response surfaces relating (a) pH *vs*. buffer concentration; (b) pH *vs*. preconcentration flow rate and (c) buffer concentration *vs*. preconcentration flow rate. Experimental conditions: sampling volume, 20.0 mL; Pb^{2+} concentration, 200 μg L^{-1}; eluent concentration, 1.0 mol L^{-1} HCl; adsorbent mass, 100.0 mg; elution flow rate, 4.0 mL min^{-1}.

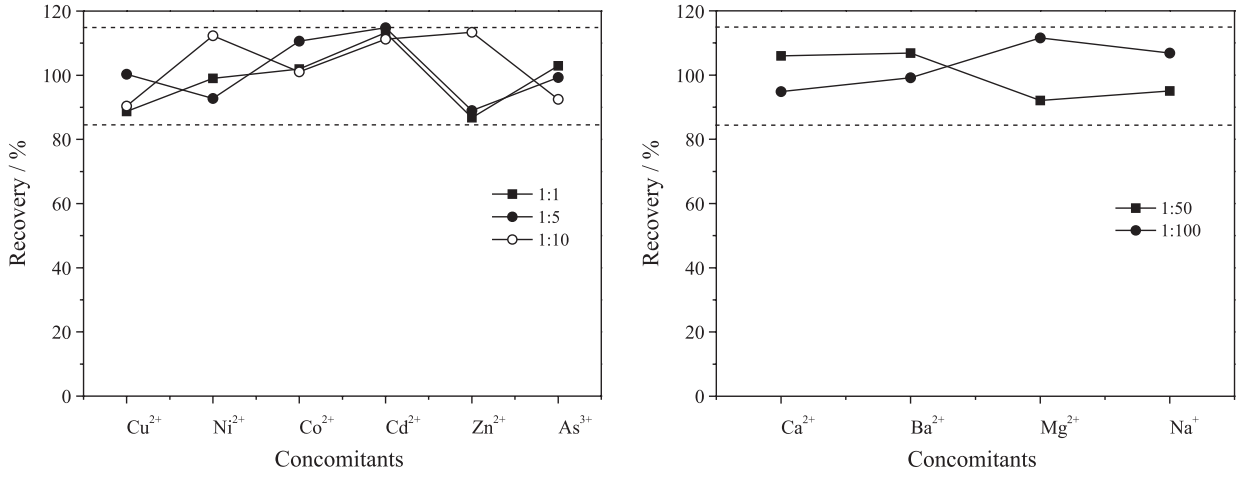

Figure 6. Recovery (%) of Pb^{2+} preconcentration in presence of concomitant ions. Experimental conditions: sampling volume, 20.0 mL; Pb^{2+} concentration, 200 μg L^{-1}; eluent concentration, 1.0 mol L^{-1} HCl; pH, 4.3; preconcentration flow rate, 4.0 mL min^{-1}; buffer concentration, 0.1 mol L^{-1}; adsorbent mass, 100.0 mg; elution flow rate, 4.0 mL min^{-1}.

Table 2. Parameters of linear regression equations and one-way ANOVA for Pb^{2+} preconcentration with SiAlSn

Linear regression equation				One-way ANOVA						
Intercept	Error	Slope / (μg^{-1} L)	Error		DF	Sum of squares	Mean square	*F*-value	*p*-value	R-adj.
				Model	1	18428	18428	1316	2.87×10^{-8}	0.99
0.034	0.002	1.62×10^{-3}	4.44×10^{-5}	Residual	6	83	14			
				Total	7	18511				

DF: degrees of freedom; *p*-value: significance of *F*-value; R-adj.: adjusted correlation coefficient.

This could be an indication to the presence of considerable binding sites capable to adsorb the lead ions in the presence of other metal ions.

Analytical features

The obtained linear regression to Pb^{2+} ions preconcentration was statistically evaluated by one-way ANOVA (Table 2). At 95% confidence level, the ratio value between the mean square of model and residual (*F*-value) was higher than the tabulated value ($F_{1,6}$ value is 5.99), indicating good model fit to the experimental data. In addition, the value of adjusted correlation coefficient (R-adj.) was equal to 0.99. Additionally, the smaller the *p*-value, the larger the significance of model, as observed from Table 2. These values indicate the impossibility of the result occurring by chance, indicating the strong relationship between absorbance and concentration values.

The acquired EF, CE, CI, AF, LOQ, LOD and range of analytical curve were determined, as shown in Table 3. The higher EF value indicates the great potentiality of online coupling of solid phase extraction using SiAlSn as adsorbent, which result in lower LOD and LOQ. The CE, which establishes the sensitivity enhancement during 1 min of preconcentration time, provides a better evaluation of procedure performance.[23] Thus, the CE was found to be 8.1 min^{-1}. The CI establishes the necessary volume (in mL) for the preconcentration system to obtain a enrichment factor.[23] AF defines the number of experiments carried out *per* hour.[24] The low LOD and LOQ values obtained also indicate a enhance on the detectabiliy by online preconcentration when compared to only FAAS.

The results of RSD for interday precision were found to be 10.48, 3.02 and 2.83% to the respective Pb^{2+} concentrations of 5.0, 100.0 and 400.0 μg L^{-1}. Intraday precision RSD values were 12.95, 3.15 and 3.13% to Pb^{2+} concentrations of 5.0, 100.0 and 400.0 μg L^{-1}, respectively. Those results showed a very low variation between measurements and good agreement with the nominal concentration. A comparison of the proposed method with other analytical methods previously reported in literature for the determination of Pb^{2+} by FAAS is shown in Table 4.

Table 3. Analytical features for Pb^{2+} preconcentration with SiAlSn

Parameter	Obtained value
EF	40.5
PE / min^{-1}	8.1
CI / mL	0.5
AF	12
LOQ / (μg L^{-1})	5.0
LOD / (μg L^{-1})	1.5
Range of analytical curve / (μg L^{-1})	5.0-400.0

EF: enrichment factor; PE: preconcentration efficiency; CI: consumption index; AF: analytical frequency; LOQ: limit of quantification; LOD: limit of detection.

The proposed method showed low sample volume, high EF value, good values of LOQ, LOD and linear range which assists on quantification of Pb^{2+} ions in small concentrations.

Analysis of samples

In order to assess the accuracy and applicability of the method in real samples, analyses of different kind of water samples, chocolate powder, herbal medicine sample and marine sediment (certified reference material) were carried out. As observed in Table 5, trace levels of Pb^{2+} ions were not detected in any sample. Thus, recovery tests with spiked samples were carried out to determine the accuracy. As observed, higher recoveries results (100-110%) were obtained, attesting the method applicability and accuracy without interferences. The amount of Pb^{2+} ions were also determined in certified reference (marine sediment, MESS-3) by this method (21.5 ± 1.2 μg g^{-1}, n = 3) and was statistically similar to the certified value (21.1 ± 0.7 μg g^{-1}) by Student's *t*-test with 95% confidence interval. Therefore, the method accuracy was confirmed even to sediment samples submitted to acid digestion.

Conclusions

The sol-gel synthesis of SiAlSn as new adsorbent material for Pb^{2+} preconcentration found to be an interesting

Table 4. Comparison of literature methods and the present method for determination of Pb^{2+} ions

Adsorbent	Preconcentration technique	Sample volume / mL	EF	LOD / (μg L^{-1})	LOQ / (μg L^{-1})	Linear range / (μg L^{-1})	Reference
Graphene	SPE (online pre-concentration)	100.0	125.0	0.6	2.0	10.0-600.0	49
Poly(AGE/IDA-*co*-DMAA-grafted silica gel	SPE (online pre-concentration)	100.0	3.4	3.5	11.7	–	50
Multiwall carbon nanotubes	SPE (online pre-concentration)	20.0	44.2	2.6	8.6	8.8-775.0	35
Restricted-access carbon nanotubes	SPE (online pre-concentration)	2.0	5.5	2.1	7.0	7.0-260.0	51
Surfactant mediated solid phase extraction combined with Fe_3O_4 nanoparticle	SM-SPE (batch assays)	10.2	25.0	0.7	ca. 2.5	1.0-10.0	52
Magnetic metal organic frameworks adsorbent modified with mercapto groups	SPE (batch assays)	10.0	100.0	0.3	ca. 1.0	1.0-20.0	53
Mercaptobenzothiazole impregnated Amberlite XAD-1180 resin	SPE (online pre-concentration)	100.0	20.0	5.0	16.5	–	54
SiAlSn	SPE (online pre-concentration)	20.0	40.5	1.5	5.0	5.0-400.0	this work

Poly(AGE/IDA-*co*-DMAA: poly[1-(*N*,*N*-bis carboxymethyl)amino-3-allylglycerol-codimethylacrylamide]; SPE: solid-phase extraction; SM-SPE: surfactant mediated solid phase extraction; EF: enrichment factor; LOD: limit of detection; LOQ: limit of quantification.

Table 5. Pb^{2+} addition/recovery test to different kind of samples (n = 3)

Sample	Concentration added / (μg L^{-1})	Concentration found ± SD / (μg L^{-1})	Recovery / %
Mineral water	0.0	ND	
	8.0	8.2 ± 0.1	103
Tap water	0.0	ND	
	8.0	8.8 ± 0.1	110
Lake water[a]	0.0	ND	
	8.0	8.8 ± 0.1	110
Ginkgo biloba powder / (μg g^{-1})	0.0	ND	
	4.3	4.3 ± 0.1	100
Chocolate powder / (μg g^{-1})	0.0	ND	
	6.0	6.1 ± 0.1	102

[a]Located in Londrina, Paraná, Brazil. SD: standard deviation; ND: not detected.

approach. Significative improvements in detectability of lead ions were achieved due to the high enrichment factor (40.5) and low consumption index (0.5 mL), yielding a low limit of detection with low sample consumption (20.0 mL). Moreover, in a reduced analysis time, the method proved to be simple, low cost (dispenses the use of chelating or organic solvents in the flow system) and selective. Due to these attractive advantages and accuracy, the method could be used for determining Pb^{2+} ions at trace levels in water, herbal medicine and food samples. Therefore, the SiAlSn can be considered an efficient alternative as a silica-based adsorbent to be utilized for preconcentration and determination of Pb^{2+} at trace levels.

Acknowledgments

This work was financially supported by Conselho Nacional de Desenvolvimento Científico e Tecnológico (CNPq), Coordenação de Aperfeiçoamento de Pessoal de Nível Superior (CAPES), INCT-BIO (FAPESP grant No. 2014/50867-3 and CNPq grant No. 465389/2014-7) and Fundação de Amparo à Pesquisa do Estado do Rio de Janeiro (FAPERJ). Also, the authors would like to thank the LMEM (Laboratório de Microscopia Eletrônica) from State University of Londrina (UEL) by having done the SEM and EDS analysis, and the ESPEC from State University of Londrina (UEL) for the FTIR analysis.

References

1. Zietz, B.; Vergara, J. D.; Kevekordes, S.; Dunkelberg, H.; *Sci. Total Environ.* **2001**, *275*, 19.
2. Tong, S.; Schinding, Y. E.; Prapamontol, T.; *Bull. W. H. O.* **2000**, *79*, 1068.
3. Health Canada; *Final Human Health State of the Science Report on Lead*; Health Canada: Ottawa, Canada, 2013. Available at http://www.hc-sc.gc.ca/ewh-semt/pubs/contaminants/dhhssrl-rpecscepsh/index-eng.php, accessed in March 2017.

4. Reilly, C.; *Metal Contamination of Food: Its Significance for Food Quality and Human Health*, 3rd ed.; Blackwell Science Ltd.: Oxford, UK, 2002.
5. Teixeira, V. G.; Coutinho, F. M. B.; Gomes, A. S.; *Quim. Nova* **2004**, *27*, 754.
6. World Health Organization (WHO); *Lead in Drinking-Water*; WHO: Geneva, Switzerland, 2011. Available at http://www.who.int/water_sanitation_health/dwq/chemicals/lead.pdf, accessed in March 2017.
7. World Health Organization (WHO); *Evaluation of Certain Food Additives and Contaminants*; WHO: Geneva, Switzerland, 2011. Available at http://apps.who.int/iris/bitstream/10665/44515/1/WHO_TRS_960_eng.pdf, accessed in March 2017.
8. World Health Organization (WHO); *Safety Evaluation of Certain Food Additives and Contaminants*; WHO: Geneva, Switzerland, 2011. Available at http://apps.who.int/iris/bitstream/10665/44521/1/9789241660648_eng.pdf, accessed in March 2017.
9. Ministério da Saúde; Portaria No. 2.914, de 12 de dezembro de 2011, *Dispõe sobre os Procedimentos de Controle e de Vigilância da Qualidade da Água para Consumo Humano e seu Padrão de Potabilidade*; Brasília, DF, Brazil, 2011. Available at http://bvsms.saude.gov.br/bvs/saudelegis/gm/2011/prt2914_12_12_2011.html, accessed in March 2017.
10. Ministério do Meio Ambiente, Conselho Nacional do Meio Ambiente (CONAMA); Resolução No. 357, de 17 de março de 2005, *Dispõe sobre a Classificação dos Corpos de Água e Diretrizes Ambientais para o seu Enquadramento, bem como Estabelece as Condições e Padrões de Lançamento de Efluentes, e Dá Outras Providências*; CONAMA: Brasília, DF, Brazil, 2005. Available at http://www.mma.gov.br/port/conama/res/res05/res35705.pdf, accessed in March 2017.
11. Ministério da Saúde, Agência Nacional de Vigilância Sanitária (ANVISA); Resolução - RDC No. 42, de 29 de agosto de 2013, *Dispõe sobre o Regulamento Técnico MERCOSUL sobre Limites Máximos de Contaminantes Inorgânicos em Alimentos*, ANVISA: Brasília, DF, Brazil, 2013. Available at http://bvsms.saude.gov.br/bvs/saudelegis/anvisa/2013/rdc0042_29_08_2013.html, accessed in March 2017.
12. EFSA Panel on Contaminants in the Food Chain (CONTAM); *EFSA J.* **2010**, *8*, ID 1570. DOI 10.2903/j.efsa.2010.1570.
13. Corazza, M. Z.; Somera, B. F.; Segatelli, M. G.; Tarley, C. R. T.; *J. Hazard. Mater.* **2012**, *243*, 326.
14. Duyck, C.; Miekeley, N.; da Silveira, C. L. P.; Aucélio, R. Q.; Campos, R. C.; Grimberg, P.; Brandão, G. P.; *Spectrochim. Acta, Part B* **2007**, *62*, 939.
15. Shamspur, T.; Sheikhshoaie, I.; Mashhadizadeh, M. H.; *J. Anal. At. Spectrom.* **2005**, *20*, 476.
16. Praveen, R. S.; Daniel, S.; Rao, P. T.; *Talanta* **2005**, *66*, 513.
17. Rao, T. P.; Daniel, S.; Gladis, J. M.; *Trends Anal. Chem.* **2004**, *23*, 28.
18. Tarley, C. R. T.; Ávila, T. C.; Segatelli, M. G.; Lima, G. F.; Peregrino, G. S.; Scheeren, C. W.; Dias, S. L. P.; Ribeiro, E. S.; *J. Braz. Chem. Soc.* **2010**, *21*, 1106.
19. Lemos, V. A.; Santos, M. S.; Santos, E. S.; Santos, M. J. S.; dos Santos, W. N. L.; Souza, A. S.; de Jesus, D. S.; das Virgens, C. F.; Carvalho M. S.; Oleszczuk, N.; Vale, M. G. R.; Welz, B.; *Spectrochim. Acta, Part B* **2007**, *62*, 4.
20. Sharma, R. K.; Pant, P.; *J. Hazard. Mater.* **2009**, *163*, 295.
21. Ali, M.; *Chin. J. Chem.* **2007**, *25*, 1663.
22. Gonçalves, J. E.; Gushikem, Y.; Castro, S. C.; *J. Non-Cryst. Solids* **1999**, *260*, 125.
23. Yalçınkaya, Ö.; Kalfa, O. M.; Türker, A. R.; *J. Hazard. Mater.* **2011**, *195*, 332.
24. Souza, E. S.; Martins, A. O.; Fajardo, H. V.; Probst, L. F. D.; Carasek, E.; *J. Hazard. Mater.* **2009**, *166*, 455.
25. Camel, V.; *Spectrochim. Acta, Part B* **2003**, *58*, 1177.
26. Marestoni, L. D.; Sotomayor, M. D. P. T.; Segatelli, M. G.; Sartori, L. R.; Tarley, C. R. T.; *Quim. Nova* **2013**, *36*, 1194.
27. Wutke, N. B.; Diniz, K. M.; Corazza, M. Z.; de Oliveira, F. M.; Ribeiro, E. S.; Fonseca, B. T.; Segatelli, M. G.; Tarley, C. R. T.; *Anal. Lett.* **2016**, *49*, 723.
28. Tarley, C. R. T.; Lima, G. F.; Nascimento, D. R.; Assis, A. R. S.; Ribeiro E. S.; Diniz, K. M.; Bezerra, M. A.; Segatelli, M. G.; *Talanta* **2012**, *100*, 71.
29. Greenwood, N. N.; Earnshaw, A.; *Chemistry of the Elements*, 2nd ed.; Elsevier Butterworth-Heinemann: Oxford, UK, 1997.
30. Sheng, T. C.; Kirszensztejn, P.; Bell, T. N.; Gay, I. D.; *Catal. Lett.* **1994**, *23*, 119.
31. Cardoso, W. S.; Francisco, M. S. P.; Lucho, A. M. S.; Gushikem, Y.; *Solid State Ionics* **2004**, *167*, 165.
32. Rejani, P.; Radhakrishnan, A.; Beena, B.; *Int. J. Chem. Eng. Appl.* **2014**, *5*, 244.
33. Currie, L. A.; *Anal. Chim. Acta* **1999**, *391*, 105.
34. Souza, J. M. O.; Tarley, C. R. T.; *Environ. Anal. Chem.* **2009**, *89*, 489.
35. Barbosa, A. F.; Segatelli, M. G.; Pereira, A. C.; Santos, A. S.; Kubota, L. T.; Luccas, P. O.; Tarley, C. R. T.; *Talanta* **2007**, *71*, 1512.
36. Lemos, V. A.; David, G. T.; *Microchem. J.* **2010**, *84*, 42.
37. *Statistica 7.0*, Statsoft, Tulsa, OK, USA, 2004.
38. *Origin Pro 8 SR0*, OriginLab Corporation, Northampton, MA, USA, 2007.
39. Lima, G. F.; Ohara, M. O.; Clausen, D. N.; Nascimento, D. R.; Ribeiro, E. S.; Segatelli, M. G.; Bezerra, M. A.; Tarley, C. R. T.; *Microchim. Acta* **2012**, *178*, 61.
40. Lima, G. F.; Ferreira, V. S.; Godoy, N. V.; Medeiros, R. F.; Garrido, F. M. S.; Ribeiro, E. S.; Nakagaki, S.; Segatelli, M. G.; Bezerra, M. A.; Tarley, C. R. T.; *Microchem. J.* **2013**, *109*, 98.
41. Costa, L. M.; Ribeiro, E. S.; Segatelli, M. G.; do Nascimento, D. R.; de Oliveira, F. M.; Tarley, C. R. T.; *Spectrochim. Acta, Part B* **2011**, *66*, 329.

42. Brigante, M.; Parolo, M. E.; Schulz, P. C.; Avena, M.; *Powder Technol.* **2014**, *253*, 178.
43. Dados, A.; Paparizou, E.; Eleftheriou, P.; Papastephanou, C.; Stalikas, C. D.; *Talanta* **2014**, *121*, 127.
44. Diniz, K. M.; Gorla, F. A.; Ribeiro, E. S.; do Nascimento, M. B. O.; Corrêa, R. J.; Tarley, C. R. T.; Segatelli, M. G.; *Chem. Eng. J.* **2014**, *239*, 233.
45. Tarley, C. R. T.; Rodrigues, T. M.; Gorla, F. A.; Germiniano, T. O.; Alves, J. C.; Inagaki, C. S.; Paschoal, V. H.; Alfaya, A. A. S.; Segatelli, M. G.; *J. Braz. Chem. Soc.* **2014**, *25*, 2054.
46. Thommes, M.; Kaneko, K.; Neimark, A. V.; Olivier, J. P.; Rodriguez-Reinoso, F.; Rouquerol, J.; Sing, K. S. W.; *Pure Appl. Chem.* **2015**, *87*, 1051.
47. Ferreira, S. L. C.; Bezerra, M. A.; Santos, W. N. L.; Neto, B. B.; *Talanta* **2003**, *61*, 295.
48. Teófilo, R. F.; Ferreira, M. M. C.; *Quim. Nova* **2006**, *29*, 338.
49. Wang, Y.; Gao, S.; Zang, X.; Li, J.; Ma, J.; *Anal. Chim. Acta* **2012**, *716*, 112.
50. Panahi, H. A.; Morshedian, J.; Mehmandost, N.; Moniri, E.; Galaev, I. Y.; *J. Chromatogr. A* **2010**, *1217*, 5165.
51. Barbosa, V. M. P.; Barbosa, A. F.; Bettini, J.; Luccas, P. O.; Figueiredo, E. C.; *Talanta* **2016**, *147*, 478.
52. Jalbani, N.; Soylak, M.; *Ecotoxicol. Environ. Saf.* **2014**, *102*, 174.
53. Wang, Y.; Chun, H.; Tang, J.; Ye, G.; Ge, H.; Hu, X.; *Food Chem.* **2015**, *181*, 191.
54. Tokalıoğlu, S.; Papak, A.; Kartal, S.; *Arab. J. Chem.* **2017**, *10*, 19.

Submitted: September 17, 2017
Published online: December 5, 2017